symmetry

MDPI

Review

Observational and Energetic Properties of Astrophysical and Galactic Black Holes

Bakhtiyor Narzilloev [1,2,3,4] and Bobomurat Ahmedov [1,5,6,*]

[1] Ulugh Beg Astronomical Institute, Astronomy Street 33, Tashkent 100052, Uzbekistan
[2] College of Engineering, Akfa University, Milliy Bog' Street 264, Tashkent 111221, Uzbekistan
[3] Institute of Engineering Physics, Samarkand State University, University Avenue 15, Samarkand 140104, Uzbekistan
[4] Tashkent Institute of Irrigation and Agricultural Mechanization Engineers, Kori Niyoziy, 39, Tashkent 100000, Uzbekistan
[5] Institute of Fundamental and Applied Research, National Research University TIIAME, Kori Niyoziy 39, Tashkent 100000, Uzbekistan
[6] Faculty of Physics, National University of Uzbekistan, Tashkent 100174, Uzbekistan
* Correspondence: ahmedov@astrin.uz

Abstract: The work reviews the investigation of electromagnetic, optical, and energetic properties of astrophysical and galactic black holes and surrounding matter. The astrophysical applications of the theoretical models of black hole environment to the description of various observed phenomena, such as cosmic rays of the ultra-high-energy, black hole shadow, gravitational lensing, quasinormal modes, jets showing relativistic effects such as the Doppler beaming, thermal radiation from the accretion discs, quasiperiodic oscillations are discussed. It has been demonstrated that the observational data strongly depends on the structure and evolution of the accretion disk surrounding the central black hole. It has been shown that the simulated images of supermassive black holes obtained are in agreement with the observational images obtained by event horizon telescope collaboration. High energetic activity from supermassive black holes due to the magnetic Penrose process discussed in the work is in agreement with the highly energetic cosmic rays observed. The astronomical observation of black holes provides rich fundamental physics laboratories for experimental tests and verification of various models of black hole accretion and different theories of gravity in the regime of strong gravity.

Keywords: black holes; accretion disk; gravitational lensing; QPOs; black hole shadow; Penrose process; Blandford-Znajek process

PACS: 04.20.-q; 04.50.+h; 04.70.-s; 04.70.Bw; 04.50.-h

Citation: Narzilloev, B.; Ahmedov, B. Observational and Energetic Properties of Astrophysical and Galactic Black Holes. *Symmetry* **2023**, *15*, 293. https://doi.org/10.3390/sym15020293

Academic Editor: Kazuharu Bamba

Received: 7 December 2022
Revised: 3 January 2023
Accepted: 16 January 2023
Published: 20 January 2023

1. Introduction

Black hole solutions for the first time were obtained by Schwarzschild in 1916 from Einstein field equations. It was shown by Oppenheimer-Snider and independently by Datta in 1939 that a black hole can be formed as a result of the gravitational collapse of a spherical massive dust object. According to Schwarzschild's solution massive objects with a total mass M collapsed below their gravitational radius $r_g = 2GM/c^2$ are conventionally called black holes (BHs). The "black" characteristic is suitable since it is supported by the observed luminosity of the hot surface of such an object, as shown by measurements of a distant observer, which decreases exponentially with time. Decrease time in e times is very small, namely $3^{3/2} r_g/(2c) \simeq 2.6 \times 10^{-5}(M/M_\odot)$ second. The discreteness of energy means that the number of emitted photons is finite, that is, even an exponential decrease in luminosity will not last forever. A "hole" notation originated from the justified assumption that neither matter nor radiation falling into such an object can escape from it after crossing

a certain critical hypothetical surface called an event horizon. This surface is spherical and has a radius r_g for the static gravitational collapsed object.

General Relativity (GR) shows that the asymptotically external field of a black hole is completely determined by its total mass M, charge Q, and angular momentum $\vec{J}$. In fact, for a classical black hole only the conserved quantities M, Q, and $\vec{J}$ are available to the outside world from all the quantities possibly characterizing the isolated source of gravitational and electromagnetic fields. It may be recalled that the above-mentioned BH quantities can be represented, according to the Gauss theorem, in terms of flows through closed surfaces. In contrast to them, this is impossible, to say, for the baryon number. To determine it, one will need to plunge into a black hole and count the particles, but these results will definitely be not available and useless to anyone outside.

For many decades black holes were considered purely mathematical objects due to a lack of observational data. However, due to the recent development of observational relativistic astrophysics black holes, which are extremely massive and fascinating astrophysical objects, are currently of great interest to scientists. These compact objects, located at the centers of galaxies, are known for their immense mass and beauty. Despite being the darkest objects in the cosmos, black holes are incredibly luminous in their immediate vicinity and have the ability to warp spacetime and heat surrounding matter to emit powerful X-rays and cosmic particles. Advances in space observatories and ground-based experimental facilities have allowed for direct and indirect confirmation of their existence in nature.

The advanced development of the angular resolution of radio observations in submillimeter wavelength due to Very Long Baseline Interferometry (VLBI) has reached the angular sensitivity to observe supermassive black holes (SMBHs). The recent triumphal observations of shadows of M87* and Sgr A* [1,2] supermassive black holes are intensively focused by international scientific collaborations, mainly by the Event Horizon Telescope (EHT) and the Black Hole Camera (BHC), aiming at VLBI observations at 1.3 mm and 0.87 mm of Sgr A* and M87* images. The angular size is estimated as $\sim$10 μat a distance of 8 kpc from the Solar System. Accordingly, the angular size of the shadow of SMBH Sgr A* is around $\sim$50 μas. The central object in the M87 elliptical galaxy has the angular size of the shadow around $\sim$40 μas based on an estimated mass of $6.4 \times 10^9 M_\odot$ and a distance of 16 Mpc.

A bright asymmetric ring surrounding a dark central region is a key feature of the SMBH images observed by EHT. The observed images of M87* and Sgr A* SMBHs are in the range of expected theoretical predictions for a rapidly rotating Kerr black hole made in the framework of the Einstein's general relativity (GR). These important observations strongly confirm the existence of black holes in nature (a key prediction of GR theory) and provide a novel powerful tool to test Einstein's GR theory in its extremely strong field regime. The Event Horizon Telescope has observed the SMBH shadows which encode useful information on the nature of the black holes observed and the spacetime geometry in the close vicinity of the event horizon. A mass of $M = 6.5 \pm 0.7 \times 10^9 M_\odot$ is inferred by the EHT collaboration through comparison of the detected shadow of SMBHs M87* and SgrA* with a data set of simulated synthetic images of various black holes.

In July 2018, the IceCube Neutrino Observatory made an unprecedented discovery of extragalactic high-energy neutrinos, which led to the identification of a blazar—a galaxy containing a supermassive black hole (SMBH)—as the source. The blazar is located about 1.75 billion light-years away and has relativistic jets directed almost directly at us. High-energy neutrinos can be produced when high-energy cosmic rays interact with surrounding matter or photons.

In May–July 2018, the GRAVITY instrument on the European Southern Observatory's Very Large Telescope (VLT) made the first direct observation of material orbiting close to a black hole, on the scale of a few Schwarzschild radii. The observations, conducted in the near-infrared K-band, revealed hot flares of gas revolving around the supermassive black hole at the center of the Milky Way at about 30% of the speed of light, just outside its event

horizon. The origin and nature of these flares/hot spots around black holes is still a topic of debate.

In mid-2018, the Gravity Collaboration announced the first successful test of Einstein's General Theory of Relativity on the scale of million-solar-mass compact objects. This was based on observations of the motion of the S2-star as it closely passed the massive black hole at the center of our galaxy. The new observations also allowed astronomers to determine the mass of the black hole Sgr A* with the greatest precision to date.

For interested readers we refer to our relevant works where spacetime properties of several compact objects have been investigated [3–15].

Here we present a review of the study of the optical and energetic properties of black holes. Section 2 is devoted to describing the astrophysical application of properties of the accretion disks to extract information about the main parameters of black holes. The next Section 3 is devoted to the discussion of photons' motion around compact objects, gravitational lensing effects, quasinormal modes of regular black holes, and a rotating black hole shadow. Rotating black holes as the source of extremely high energetic activity is discussed in Section 4. The last section, 5 summarizes the scientific topics discussed in this review.

2. Analysis of Observational Properties of Accretion Disks to Extract Information about Black Hole Parameters

Astrophysical black holes (BHs) are formed at the end state of evolution of massive stars as compact objects with very strong gravity such that everything, including the light rays, that crosses the event horizon of BH never goes out. Then, one may ask "if it is so and the event horizon does not have either emission or reflection, then how it is possible to get information about them?". There are many ways to extract information from black holes but in this section, we are focused on the methods that allow getting constraints on the main characteristics of black holes based on the electromagnetic spectrum of the radiation coming from the accretion disk surrounding a central black hole. The main idea of each method is based on the reflection of the final electromagnetic spectrum radiated by the accretion disk around the black hole because astronomical observations indicate that such spectrum is strongly affected by the gravitational field of the central black hole. This in turn allows one to extract information about the main parameters of the black hole situated in the central part of the accretion disk. However, it is worth noting that such methods strongly depend on the model chosen to explain the black hole spacetime, the basic mechanism of phenomena for the method used, and the structure of the accretion disk surrounding the central black hole. One should also notice that there are various accretion disk models in the literature. For example, in [16] the authors have developed a model that describes an accretion disk that has a torus-like structure and evolves with time. General relativistic magneto-hydrodynamic (GRMHD) simulations of such a disk model have been investigated by Tashkent group members. In Figure 1 as an example, the results of GRMHD simulations of the mentioned disk model around a non-rotating Schwarzchild black hole are presented. One can clearly see from the evolution of the matter flow in the accretion disk presented in Figure 1 that accretion disk structure can change over time with considerably high speed which can in turn complexify to model the black hole environment in general.

For our purpose we mostly use the so-called Novikov-Thorne accretion disk model which is the simplest one and widely used in most analytic methods. We start here with the introduction of this popular model for the accretion disk.

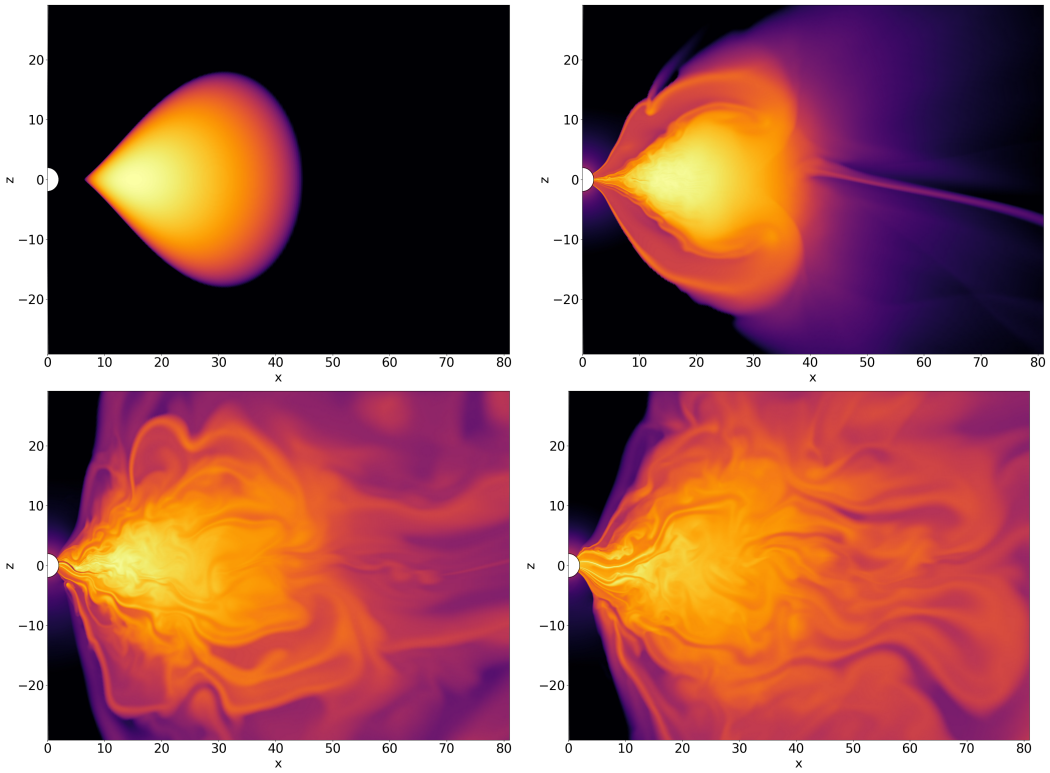

Figure 1. GRMHD simulations of a Fishbone-Moncrief model single torus [16] around a non-rotating Schwarzchild black hole. The simulation domain has 512 × 512 × 1 cells in (r, θ, ϕ), respectively. The inner edge of the torus is at the ISCO radius $6M$ and the pressure center is located at $15M$, where M is the total mass of the central black hole. The figures are captured at the cross-section of the torus in xz-plane and have time evolution from 0 to 9 periods around the black hole at the ISCO radius. Credit from Bardiev.

2.1. Novikov-Thorne Thin Accretion Disk Model

The Novikov-Thorne thin disc model [17] can be used to obtain the continuum spectrum emitted from the accretion disc of a black hole. In this model, the electromagnetic radiation emitted from the thin accretion disc generates the observed continuum spectrum. The accretion disc is geometrically thin, so particles can be considered as being mostly fixed in the equatorial plane. This means that their trajectories are mostly circular with some small radial motion. Viscous forces cause the particles to move in spiral-like trajectories, ultimately leading to their capture by the central gravitational object.

In the thin accretion disc, the gravitational force dominates over the gradients of radial pressure, causing the particles to follow circular geodesics. The strong gravitational field of the central black hole has a significant impact on the accreting matter, overwhelming any other effects on hydrodynamic, thermodynamic, and radiative processes, which can be disregarded. As particles approach the central massive object, they lose gravitational energy. This energy lost by the matter falling into the central gravitational object can be converted into energetic electromagnetic radiation. The surrounding matter partially absorbs the generated electromagnetic radiation due to the interaction and the rest escapes from the system and propagates to the asymptotic infinity. The accretion disc can be assumed as optically thick and geometrically thin without trapped heat. The temperature of the dis—the interaction of the matter and radiation defines black body electromagnetic radiation produced. The peak being responsible for soft X-ray wavelength around the astrophysical stellar-mass black holes is part of the multi-color emission spectrum (see, e.g., [17–19]). It is believed that for the thin accretion disc model, the black hole spectrum can be described with high accuracy.

2.2. Methods to Extract Information about Parameters of Central Black Hole

There are several powerful methods developed in the literature to extract information about black hole parameters from the electromagnetic spectrum of the accretion disk. We plan to discuss the most popular methods that are widely recognized by astrophysics society namely, the Continuum-Fitting Method, X-Ray Reflection Spectroscopy, Quasi-periodic Oscillations in this subsection, and Imaging Black Holes in the next section. We start our review with the first method mentioned above.

2.2.1. Continuum-Fitting Method

The study of accretion disks around black holes has been a topic of great interest in the field of Astrophysics. One of the most powerful techniques used to calculate the thermal spectrum of a thin accretion disk as detected by a distant observer is the Novikov-Thorne thin disk model. This model is based on the assumption that the space-time metric in close vicinity of the compact object is described by the Kerr black hole solution and that the inner edge of the accretion disk is located at the ISCO radius. The spin parameter of the black hole, a_*, can be measured using this technique.

The continuum-fitting method, initially proposed in the pioneering paper [20], has been widely used to estimate the spin parameter of more than ten stellar-mass black holes. This method has been extended to non-Kerr spacetime to test the space-time metric around astrophysical black holes, as can be seen in literature [21,22]. At the moment, the continuum-fitting method is considered as the most robust technique available [23,24].

Despite some of its weak points, the principles of the continuum-fitting method are relatively well understood. As such, it is a powerful tool for understanding the properties of accretion disks around black holes and for testing the predictions of the General Relativity theory. Further research in this field could help us to better understand the properties of black holes and the behavior of matter in their vicinity.

First, the possible corrections for non-black body effects may play a crucial role which is taken into account within the disk atmosphere models. However, the validity of these models is sometimes criticized.

Second, the measurement of the BH spin demands independent measurements of the total mass M of the compact object, the inclination angle of the disk i, and the distance D. The measurements of these fundamental parameters are usually obtained through optical observations. However, the uncertainty in the measurement of these quantities is usually large (eventually, the final uncertainty of the measurement of the BH spin parameter is mainly due to these uncertainties) and produced by systematic effects which are not properly controlled.

Third, the continuum-fitting method is typically used to study the properties of stellar-mass black holes. The thermal spectrum of a Novikov-Thorne disk around a central black hole with a mass of approximately $10\,M_\odot$ is in the soft X-ray band ($\sim$1 keV), while for a compact object with a total mass of 10^5–$10^{10}\,M_\odot$, the spectrum is in the optical/UV band ($\sim$1–10 eV). The measurement of the properties of supermassive black holes is limited by extinction and dust absorption, making accurate measurements difficult. The application of the continuum-fitting technique to supermassive black holes is limited to very specific cases [25,26]. The spectrum of supermassive black holes is relatively simple, without many specific features, making it possible to only measure one parameter of the near horizon geometry. In most cases, it is sufficient to measure the spin parameter of a Kerr black hole. However, this can lead to a degeneracy between the estimate of the black hole spin and possible deviations from the standard Kerr solution.

2.2.2. X-ray Reflection Spectroscopy

According to this method, the astrophysical black holes are assumed to be surrounded by hot gas having extremely high temperatures. This gas structure is called corona and together with the accretion disk the model is called the disk-corona model (see Figure 2 for illustration). The corona in the disk-corona model is a hot (T $\sim$ 100 keV), optically thin,

electron cloud that enshrouds the central disk. Inverse Compton scattering of thermal photons is emitted from the disk off free electrons in the corona which generates X-rays. A power-law spectrum is produced for the corona due to multiple inverse Compton scattering. Several configurations for the geometry of the corona have been proposed in the literature since it is unknown. The disk is also illuminated by the emission from the corona, which produces a reflected component with the known emission lines. Depending on the ionization degree of the disk surface the most interesting line is at 6.4–6.97 keV which belongs to the iron K_α one.

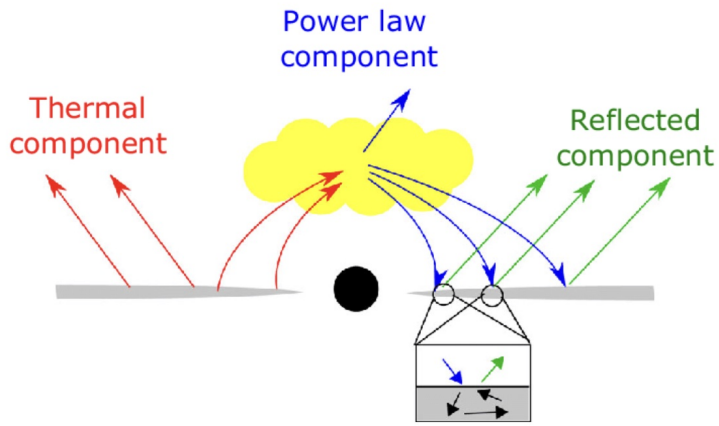

Figure 2. Schematic assumption on the disk-corona model according to [27]. The black circle is the central black hole, the accretion disk is shown with thin grey triangles, and the hot corona is shown as a cloud with yellow colour.

A powerful tool to probe the nature of the astrophysical black holes comes from the analysis of the iron K_α line which can be observed from both astrophysical SMBHs and stellar—mass and its shape does not directly depend on the gravitational mass of the object which in turn allows the technique to be applied to both BH object classes. While the whole reflection spectrum of the complex source is fitted, the spacetime properties in the vicinity of the black hole are mainly tested through the iron line analysis. So-called the iron line method to determine the black hole spin is based on the technique of fitting the reflection spectrum. In a preliminary study, a broad iron line can be added to a power-law component as a simple model and in principle can not be employed to measure a black hole spin.

Two models to describe the spectrum of supermassive BH NGC 1365 are compared in Figure 3. The absorber model demonstrated with the red line is the first one and the reflection model demonstrated with the green line is the second one. The broad iron line at 3–7 keV could be explained within both the absorber and the reflection models. However, the spectrum above 10 keV can not be fitted in the absorber model. The detailed analysis of NuSTAR data of NGC 1365 definitively supports the origin of the iron line spectrum from the reflection and rules out the absorber model. Accordingly, the reflection model is indeed a reasonable model to explain the whole X-ray spectrum of the radiation produced by black hole systems.

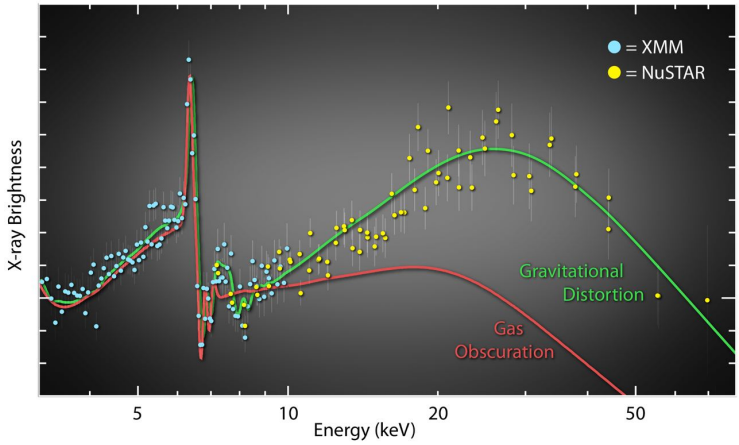

Figure 3. The AGN NGC 1365: observed data from the space X-ray telescopes XMM-Newton (blue dots) and NuSTAR (yellow dots) versus theoretical predictions based on the absorber model (red solid curve) and on the reflection model (green solid curve). The absorber and the reflection models both predict almost the same spectra for the iron line at low energies in the way that the XMM-Newton data cannot distinguish the results of the two models. However, the two models predict different spectra for the iron line at higher energies. The Compton hump at the energy range of 20–40 keV is demonstrated by the reflection model. The reflection model is supported and the absorber model is ruled out by the NuSTAR X-ray data. See [28] and the text there for more details. Adopted from NASA/JPL-Caltech/ESA/CfA/INAF.

2.2.3. Quasi-Periodic Oscillations

Quasi-periodic oscillations (QPOs) are a common property in the X-ray power density spectra (PDS) of compact neutron stars and stellar-mass black holes, as observed in [29,30]. These QPOs can be observed as relatively narrow peaks at characteristic frequencies. Among black hole binaries, high-frequency QPOs at around 100 Hz are of particular interest for several reasons:

i. The detected QPOs frequency is within the expected range for the matter orbiting nearly at the ISCO radius around the central source.
ii. The frequency of the QPOs is relatively insensitive to the properties of the accretion flow and is primarily determined by the spacetime properties. However, there is a slight dependence on the observed X-ray flux.
iii. The frequency of the QPOs can be measured with a high degree of accuracy.

Due to the mentioned properties, QPOs treatment provides a powerful tool to probe the nature of black holes for precise measurement of the BH parameters. However, up to date, the actually confirmed mechanism responsible for the production of QPOs is really not known. In the current literature there are several proposals as the relativistic precession models [31–33], the resonance models [34–36], and the diskoseismology models [37–39].

Table 1 summarizes spin measurements of the stellar-mass black hole GRO J1655-40 based on different QPO models. All models assume that the geometry around the central compact object is described by the Kerr BH solution. The source is observed to have high-frequency QPOs at 300 and 450 Hz. The relativistic precession model uses low-frequency QPOs as well and does not require knowledge of the mass of the central object as input. The diskoseismology model estimates the black hole mass and spin parameters based on the input parameters of the two high-frequency QPOs. The mass of GRO J1655-40 is known from optical observations and can be applied to measurements that require the black hole mass as an input. The results in the table demonstrate that the correct interpretation of the two QPO frequencies is crucial, and different models may provide very different values for the black hole spin. In summary, the main drawback of this method is that the underlying cause of QPOs is not fully understood. With more evidence on the mechanism behind QPOs, it would be possible to accurately measure the spin of astrophysical black holes.

Table 1. The spin measurements of gravitational object GRO J1655-40 are based on the different QPO models and assume that the spacetime geometry of the compact object is described by the standard Kerr BH solution (a_* is dimensionless spin of a black hole). The knowledge of the mass of the gravitational object is not requested for the spin measurements in the framework of the relativistic precession model and the diskoseismology model. The value range of the assumed mass adopted to infer the black hole spin is reported in the third column for the other model measurements. Adopted from [40].

Model	a_*	Assumed Mass ($M_\odot$)	References
Relativistic precession model	0.290 ± 0.003	–	[41]
Diskoseismology model	0.917 ± 0.024	–	[39]
Warp resonance model	0.9–0.99	5.1–5.7	[42]
3:2 Parametric resonance model	0.96–0.99	6.0–6.6	[43]
2:1 Forced resonance model	0.31–0.42	6.0–6.6	[43]
3:1 Forced resonance model	0.50–0.59	6.0–6.6	[43]
2:1 Keplerian resonance model	0.31–0.42	6.0–6.6	[43]
3:1 Keplerian resonance model	0.45–0.53	6.0–6.6	[43]

Our research group recently conducted a study on Quasi-Periodic Oscillations (QPOs) in black hole spacetime. The study includes various solutions and is referenced in [44–48]. One example is the examination of QPOs from black holes in symmergent gravity in reference [45].

The data in Figure 4 illustrates the range of possible values for the upper and lower frequencies of twin-peak Quasi-Periodic Oscillations (QPOs) around a symmergent gravity black hole. The graph shows the results of the RP, WD, ER2, and ER3 models. The inclined blue solid line represents the limit of twin-peak QPOs, as the two peaks occur at the same frequency. The light-blue shaded area indicates the frequency range in which twin-peak QPOs cannot be detected. It can be seen that low-frequency twin-peak QPOs do not occur due to the presence of a non-zero a parameter. For $a < 1$, frequency ratios increase slightly, but for $a > 1$, the same ratios decrease in comparison to the Schwarzschild case ($a = 1$). The ER2 and ER3 models also reveal that two distinct QPOs with similar frequency ratios could be observed for upper (lower) frequencies above 450 Hz (250 Hz). Similar frequency degeneracies are also observed at low-frequency twin-peak QPOs around 100 Hz in the RP and WD models, and between 100–200 Hz in the ER3 model.

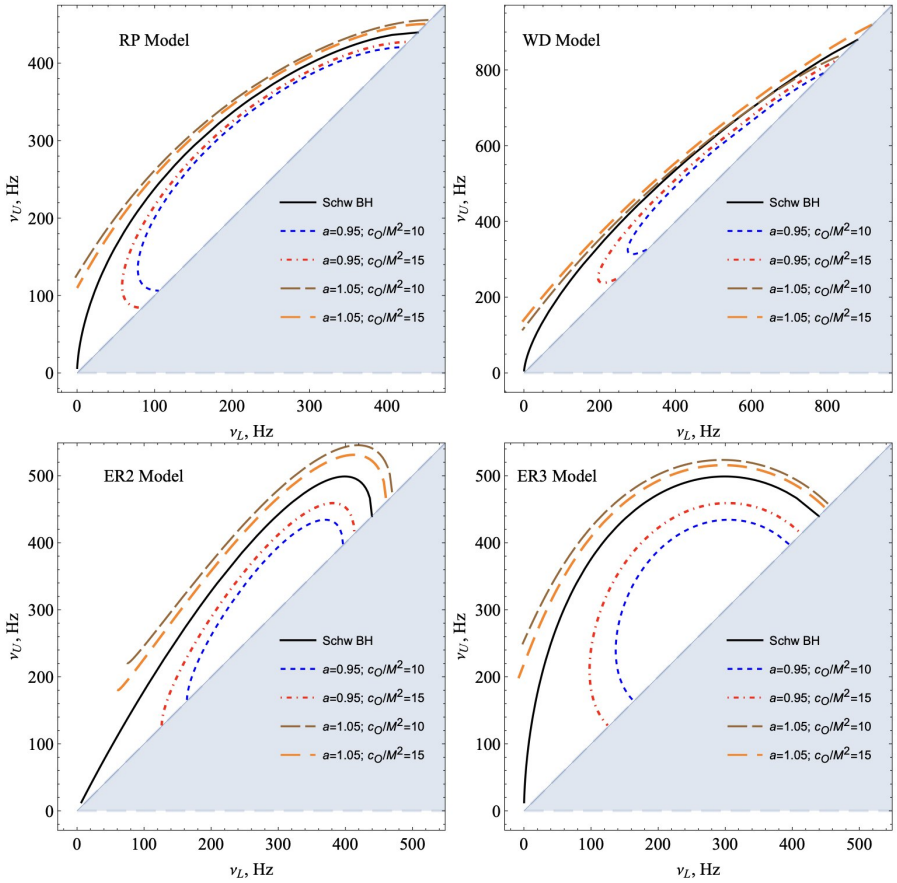

Figure 4. The graph illustrates the correlation between the upper (ν_U) and lower (ν_L) frequencies of twin-peak Quasi-Periodic Oscillations (QPOs) for a symmergent black hole with a mass of $M = 5M_\odot$. It is divided into four sections, each representing a different model: RP, WD, ER2, and ER3. These sections are displayed on a $\nu_L - \nu_U$ plane, showing the effect of symmergent gravity parameters $a = 0.95$ & 1.05 and $c_o/M^2 = 10$ & 15 on the frequency curves. The curves are distributed above and below the Schwarzschild curve, with c_o/M^2 values showing finer structures. Credit from [45].

3. Imaging, Optical and Observational Properties of Black Holes

The study of the geodesics of test particles and photons in the vicinity of black holes is of great importance in understanding the nature of these compact objects. The motion of photons around black holes has a direct connection to one of the key predictions of General Relativity (GR) concerning the bending of light in a gravitational field. The spacetime curvature around a black hole bends light and creates an effect similar to that of an optical lens, known as gravitational lensing (GL).

The first observation of GL was made during the solar eclipse of 1919 by Arthur Eddington. This groundbreaking observation provided the first experimental confirmation of GR and has since been used to study a wide range of astrophysical phenomena, including the properties of black holes and the distribution of matter in galaxies.

In this section, we present a detailed study of the geodesics of test particles and photons in the vicinity of a black hole. We focus on the effects of GL and the implications of these effects for our understanding of the properties of black holes and the nature of gravity.

We begin by providing a comprehensive overview of the theory of GL and its predictions in GR. We then present our results from numerical simulations of the geodesics of test particles and photons in the vicinity of a black hole, focusing on the effects of GL on the motion of these particles.

Our results reveal that GL plays a crucial role in the dynamics of particles and photons in the vicinity of a black hole. We find that the bending of light can lead to significant

distortions in the apparent positions of objects and can also result in multiple images of the same object. These findings have important implications for the ongoing search for new ways to probe the properties of black holes and the nature of gravity.

In conclusion, our study provides a detailed examination of the geodesics of test particles and photons in the vicinity of a black hole and the effects of GL on their motion. Our results have important implications for the ongoing quest to understand the properties of these fascinating objects and the nature of gravity.

3.1. Black Hole Shadow

Obtaining a precise observation of the accretion flows around a black hole through direct imaging can provide valuable information about the black hole's characteristics. This can be achieved by assuming that the black hole is surrounded by either an optically thin emitting medium or a Novikov–Thorne accretion disk, which would result in a dark area, known as the shadow of the black hole, being visible against a brighter background. It is important to note that this shadow is not produced in the same way as a common shadow, in which an object blocks light. Instead, when a black hole is surrounded by an optically thin emitting medium, the boundary of the shadow corresponds to the apparent photon capture sphere. This concept is described in references [49–51].

For a black hole surrounded by a Novikov–Thorne accretion disk, the boundary of the shadow corresponds to the apparent image of the Innermost Stable Circular Orbit (ISCO). In other situations, such as a black hole surrounded by an optically thick emitting medium, there may not be a shadow visible. However, if the black hole is completely surrounded by an optically thin emitting medium, its image will appear as a dark area against a bright background. This dark area is known as the black hole shadow, and its boundary corresponds to the image of the photon capture sphere as seen by a distant observer. In real observations, it is not possible to fire photons directly at a black hole and observe scattering, but such an effect can be inferred by observing the surrounding medium.

We briefly explain the main idea of the method based on that the image of the shadow of a black hole strongly depends on the spin parameter. In Figure 5 it is shown how the shadow shape and size are modified with the change of the spin of a black hole (for various viewing angles we refer the reader to [52]). It can be observed that with the increase of the BH spin, the center of the shadow shifts and the shadow takes a shape that differs from the circle. With the precise measurement of the average radius and the distortion of the shape from the circle, it is possible to get constraints on the spin of a black hole.

The method can be explained in a detailed way. Figure 6 represents the closed boundary of the BH shadow. The image is symmetric with respect to the horizontal X-axis. It is the apparent image of the photon capture sphere which differs from the image of the inner edge of the disk. The BH shadow is symmetric with respect to the X-axis and $R(0)$ is defined as the shorter segment between C and the boundary of BH shadow along the X-axis. In Figure 6 the function $R(\phi)$ defines the distance between the central point C and the boundary at the angle ϕ.

The shape of the shadow is completely described through the function $R^{obs}(\phi)/R^{obs}(0)$ which is preferable to $R(\phi)$. The latter depends on the additional two parameters the mass and the distance from the black hole which may not be known with high precision. In any case, it would be better to ignore them. Then for the BH shadow, one has the set $\{R^{obs}(\phi)/R^{obs}(0)\}$, where $\{\phi_i\}$ is a set of angles for which there are the measurements of the quantity $R^{obs}(\phi)/R^{obs}(0)$. At this stage, one could either compare two BH shadows or fit an observed shadow with a theoretical model. The theoretical model depends on the black hole parameters as the spin a_*, the viewing angle i, and a number of extra parameters p_1, p_2, etc. The observed shadow is indicated through $R^{obs}(\phi)/R^{obs}(0)$ inferring the values of the

parameters of the applied theoretical model by employing a goodness-of-fit statistical test. For instance, one may introduce the function S defined as

$$S(a_*, i, p_1, p_2, \ldots) = \sum_k \left(\frac{R(a_*, i, p_1, p_2, \ldots; \phi_k)}{R(a_*, i, p_1, p_2, \ldots; 0)} - \frac{R^{obs}(\phi_k)}{R^{obs}(0)} \right)^2 , \quad (1)$$

and find the best fit by minimizing the function S to get observable constraints on the BH parameters.

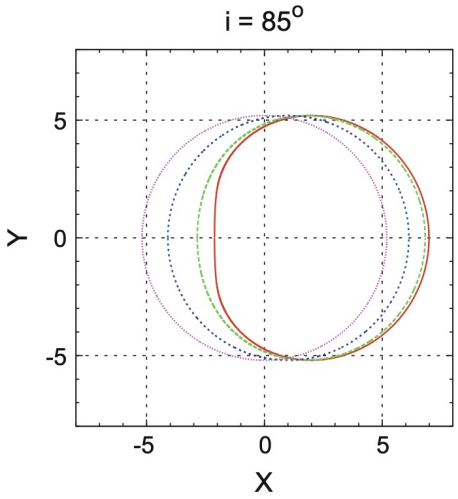

Figure 5. The figure illustrates the impact of the spin parameter a_* on the shape of the apparent photon capture sphere of a rotating Kerr black hole, when the viewing angle is fixed at $i = 85°$. The figure shows the different shapes of the photon capture sphere for the following values of the BH spin parameter: $a_* = 0$ (magenta dotted curve), $a_* = 0.5$ (blue dotted curve), $a_* = 0.9$ (green dashed curve), and $a_* = 0.998$ (red solid curve). As the spin parameter increases, the shape of the photon capture sphere becomes more distorted. Credit from [53].

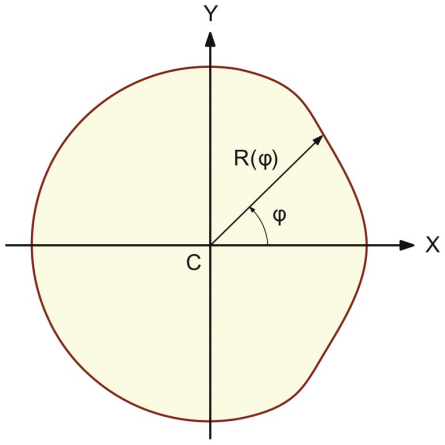

Figure 6. The closed boundary of the shadow in the polar coordinates depends on the angle ϕ. The function $R(\phi)$ defines the distance from the center C (From [53], see also [54]). See the text for more details.

The weakness of this method is that currently there is no telescope that can take a picture of a black hole with high resolution and the images of supermassive black holes obtained by EHT are not accurate enough to get precise measurements of BH parameters. For this reason, one may conclude that this methodology is currently in progress and would be available in the near future when the network of more powerful radio telescopes with high accuracy will be established.

In GR group in Uzbekistan the extensive study on this direction is performed [55,56] and recently a TM code to simulate the BH image as presented in Figures 7 and 8 has been developed. As can be seen from Figure 8 the simulated images obtained by our code show somewhat similar results obtained by the EHT consortium. As the next step, we are planning to develop a code to make corresponding data fitting process to get constraints on black hole spacetime parameters.

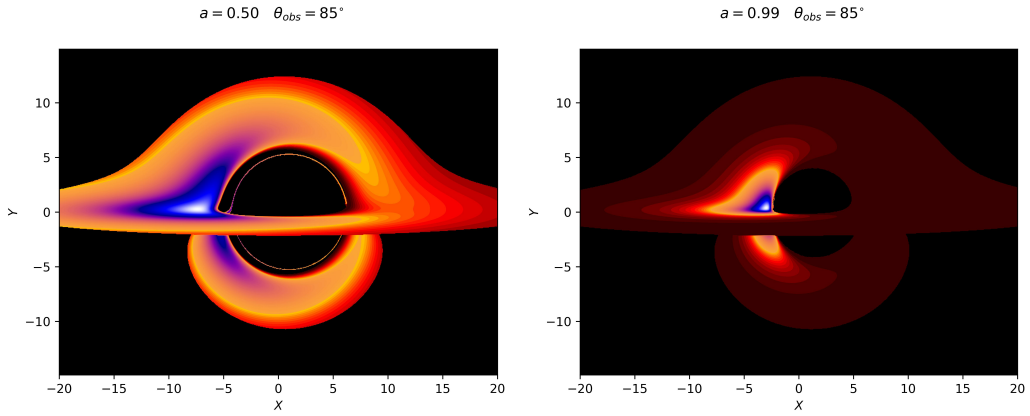

Figure 7. Simulated synthetic images of a black hole shadow formed due to the light emitted from the thin accretion disk around a rapidly rotating Kerr black hole. One can see the strong dependence on the size and shape of the rotating black hole shadow from the spin parameter. Credit from Mirzaev.

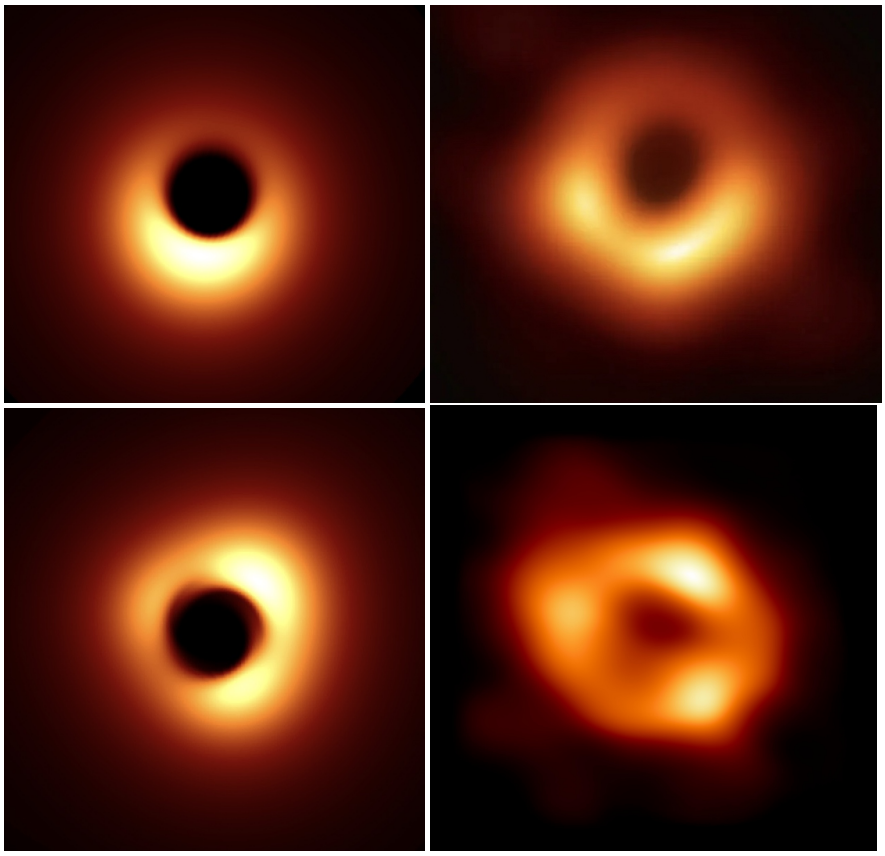

Figure 8. Simulated images of supermassive black holes assuming that their spacetime is described by the Kerr solution in the center of the elliptic galaxy M87 (**top left**) and in our local galaxy Milky Way (**bottom left**) together with the corresponding observed images of M87* and Sgr A* by the EHT consortium (**top right** and **bottom right**). Credit from Mirzaev (**left panels**) and [1,2] (**right panels**).

There are other powerful techniques to probe the nature of SMBHs as well. For example, so-called reverberation mapping is applied to measure the mass of SMBHs. It is based on the analysis of the structure of the broad-line region around an SMBH at the AGN. It is usually treated as an estimation of the mass method. Accordingly, the central mass is measured through the value of gravitational force acting on the surrounding gas around SMBH [57].

3.2. Gravitational Lensing by Black Holes

Gravitational lensing is a phenomenon that occurs when the gravitational field of a massive object bends and distorts light, causing it to follow a curved path. This can lead to a number of interesting phenomena, such as the formation of multiple images of a distant object or the magnification of distant objects. Black holes are particularly interesting objects for studying gravitational lensing because of their extreme gravitational fields and their compact size.

One of the most well-known examples of gravitational lensing by a black hole is the Einstein ring, which is a circular image of a distant object that forms around a black hole. This occurs when the gravitational field of the black hole bends the light from the distant object in such a way that it forms a complete circle around the black hole. The Einstein ring is a unique feature of gravitational lensing by black holes and is a direct consequence of the strong gravitational field of the black hole.

In addition to the formation of Einstein rings, black holes can also produce multiple images of a distant object. This occurs when the light from the distant object is bent around the black hole in such a way that it reaches the observer along multiple paths. The observer will then see multiple copies of the same object, each one slightly offset from the others due to the different paths taken by the light. Our study, as outlined in reference [58], demonstrates the formation of Einstein rings around compact objects that possess magnetization, in an environment containing plasma. This is depicted in the left panel of Figure 9.

Gravitational lensing by black holes can also lead to the magnification of distant objects. This occurs when the light from the distant object is focused by the gravitational field of the black hole, causing it to appear brighter to the observer. This can be used to study distant objects that would otherwise be too faint to observe, and it has led to some of the most distant and faint objects ever detected. The right panel of Figure 9 illustrates the comparison of various magnification levels for an image source when viewed through a compact object with magnetization and in a plasma environment. The upper and lower "solid" lines represent the scenario in which there is no magnetic field present in the plasma, while the dashed and dotted-dashed lines demonstrate the deviation from this caused by the presence of a homogeneous plasma and the "Zeemann" effect, respectively. (Please refer to reference [58] for a more detailed explanation).

In addition to its role in the study of distant objects, gravitational lensing by black holes has also been used to test general relativity and to study the properties of black holes themselves. For example, the gravitational field of a black hole can be used to test the predictions of general relativity and to search for deviations from this theory. Additionally, the study of gravitational lensing by black holes has provided important insights into the nature of these objects and their role in the universe.

Overall, gravitational lensing by black holes is a fascinating and important area of study that has led to many important discoveries and has the potential to continue to provide new insights into the nature of black holes and the universe as a whole.

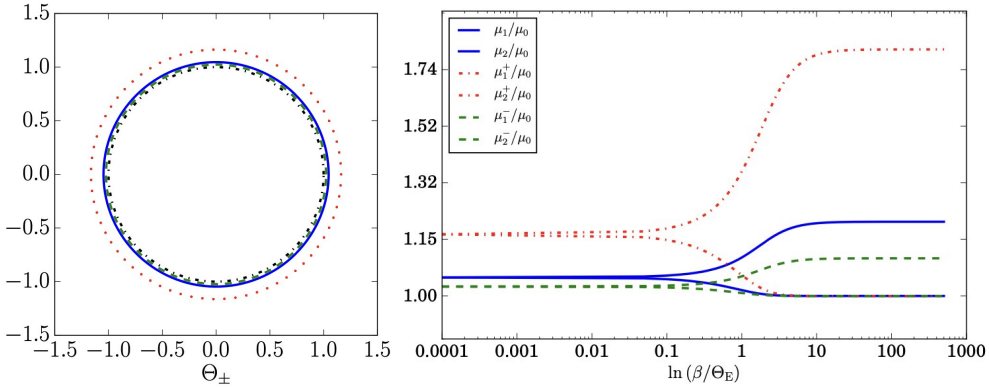

Figure 9. In the left panel of the figure, we show the Einstein ring for the plasma frequency $\omega_0 = 0.4\omega$ and the cyclotron frequency $\omega_c = 0.6\omega$. The black line represents the case in a vacuum, and the blue line represents the situation where plasma is present. In the right panel, we depict the ratio of magnification as a function of β/Θ_E. Additional information can be found in reference [58].

3.3. Quasinormal Modes of Regular Black Holes

Quasinormal modes (QNMs) are a characteristic feature of black holes and other compact objects. They are complex frequencies that describe the oscillations of fields (such as the gravitational field) around a black hole. The real part of the frequency describes the oscillation frequency, while the imaginary part describes the rate at which the oscillation decays. QNMs are important because they can provide information about the properties of a black hole, such as its mass and angular momentum.

In the case of regular black holes, QNMs have been studied extensively in the context of alternative theories of gravity. Regular black holes are a class of black holes that are proposed to exist in some alternative theories of gravity, such as modified gravity or non-singular black hole models. These theories attempt to modify the singularity at the center of a black hole, which is a point of infinite density and curvature, to a regular, non-singular object. This can be done by introducing new fields or modifying the Einstein field equations.

One of the main challenges in studying QNMs of regular black holes is that these objects are not well understood and there is no consensus on their exact properties. Therefore, it is difficult to make precise predictions about their QNMs. However, several approaches have been proposed to study QNMs of regular black holes. One approach is to use perturbation theory, which involves solving the equations of motion for small perturbations around a black hole. This can provide insight into the behavior of QNMs for a given black hole model.

Another approach is to use numerical methods, such as the finite element method or the pseudospectral method, to solve the equations of motion for a black hole. This can provide more accurate predictions for the QNMs of a black hole, but it is a more computationally intensive approach.

Despite the challenges, there have been a number of studies that have attempted to calculate the QNMs of regular black holes. These studies have found that the QNMs of regular black holes can be significantly different from those of singular black holes. For example, the QNMs of regular black holes may have a different frequency dependence on the mass and angular momentum of the black hole, and they may also have a different behavior in the low-frequency limit.

Our study (reference [59]) shows that Figure 10 illustrates how electromagnetic perturbations evolve over time in both NED Maxwellian regular black holes and RN black holes. As shown in Figure 10, the main difference in how electromagnetic perturbations behave in black holes with linear and nonlinear electrodynamics is that increasing the charge parameter in NED Maxwellian regular black holes prolongs the duration of perturbations, while in linear electrodynamics it shortens the lifetime of the electromagnetic perturbations.

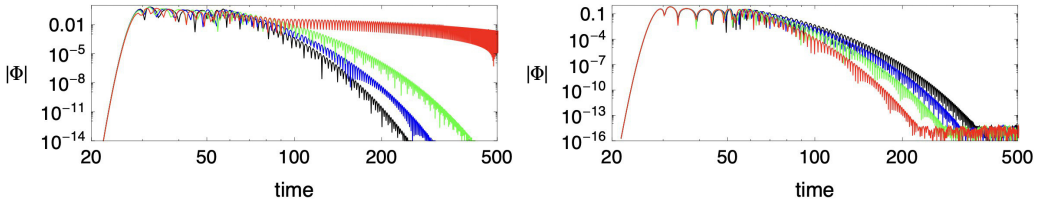

Figure 10. The figure displays the evolution in time of the fundamental modes of the electromagnetic perturbations for Maxwellian regular black holes (**left panel**) and RN black holes (**right panel**) for various values of charge parameter $Q = 0.2$ (black), $Q = 0.6$ (blue), $Q = 0.8$ (green), and $Q = 0.998$ (red). Additional information can be found in reference [59].

Overall, the study of QNMs of regular black holes is an active area of research that can provide insight into the properties of these objects and the theories of gravity that describe them. While there is still much that is unknown about regular black holes, the study of their QNMs can help to shed light on their nature and may provide a way to test these theories experimentally.

4. Black Hole Energetics

4.1. High Energetic Activity from Rapidly Rotating BHs

The physics behind the emission of jets and their formation is universal and common in nature. Jets are relevant to compact black holes and neutron stars but also to extended young proto- and newly born stars, where the typical velocity of the outflowing matter is very far from being ultra-relativistic. A common property in nature is the accretion of matter onto a gravitational object. Moreover, the presence of accretion disks around gravitational objects unambiguously indicates that the incident matter has a large angular momentum. It is very clear that the only mechanism capable of explaining the high energetics of compact objects is the release of gravitational energy that is, simply potential energy when matter falls on a compact object. Accretion is the most powerful source of energy realized in Nature, which can produce a huge energy output (Of course annihilation of electron-positron pairs can produce 100% but the amount of energy released is negligibly small). When accreting matter falls down onto the surface of a relativistic neutron star or event horizon of a black hole up to 10% of mc^2 can be released which was originally suggested by Zel'dovich and Salpeter in [60,61] in 1964 in the independent way. Therefore, to explain the high energetic activity of compact massive objects (which indicates the sufficiently high rate of accretion of matter), it was important to look for an effective process for diverting the extra angular momentum outwards the accretion disk limits. Apparently, jet emissions play precisely this role.

A reasonable trustable model of the machine at the center is based on an explanation of the different issues. It is important to explore (i) the evaluation of compact gravitational object for the maximum value of the total energy loss, (ii) the efficient mechanism of transfer of the extra angular momentum from the accreting matter into the jet emitted, and (iii) the mechanisms for the jet emissions collimation. At present, in the literature there is no proper way to cover the above issues altogether. Therefore, here we plan to discuss energy extraction from a rapidly rotating black hole which coincides with the main objectives of the review. It is strongly believed that the energetics of active galactic nuclei, in microquasars and sources of highly energetic gamma-ray bursts, are related to the central black holes. It seems the strong electric currents occurring in the plasma magnetosphere of a rotating black hole are responsible for the mechanisms of energy loss from these objects, which transform the kinetic energy into the electromagnetic radiation.

Alternatively, hard gamma rays can be generated by the process of collision of relativistic particles initially generated in the plasma magnetosphere of a black hole with optical and X-ray photons emitted by a disk due to the inverse Compton effect. This is a prominent method of Compton boosting to achieve very high energy radiation (TeV)

sources. The generation of electron-positron pairs filling the magnetosphere of a black hole can be also performed through the collision of hard gamma rays with other photons.

Consequently, the jet emissions from a black hole should consist of electron-positron plasma in contrast to the typical electron-ion plasma produced in an accretion disk. No emission lines emitted by ordinary matter are observed in relativistic emissions of micro-quasars which justifies this model. On other hand, the possible existence of ultra-relativistic protons with huge energy in the flow from sources of gamma-ray bursts contradicts the total energy release of the gamma-ray burst which is a strong limitation on the electron-positron composition in the jet emission. Overall estimations indicate that the contribution of protons can be only of the order of 10^{-5} of the total number of charged particles. Consequently, jets from black holes are composed of electron-positron plasma only.

The spin of the black hole can be powered by an accreting matter with its own angular momentum which will increase the angular velocity of rotation of the central engine. The black hole can spin up to the extremality limit of $\Omega_H r_h \sim c$ i.e., the rapidly rotating extreme Kerr black holes are powered by accretion. It is strongly believed that the millisecond radio pulsars are powered by accretion which justifies the effectiveness of this process. Therefore, the gravitational energy of the incident matter together with the kinetic energy of rotation of the black hole is the source of the high energetic activity. For the supermassive black hole (SMBH) with mass $10^9 M_\odot$ the rest energy $\mathcal{E}_{rot} \approx Mc^2$ is of the order of 10^{63}erg and comparable to the kinetic energy of rotation. The total energy reserved is well enough to explain the observed energy release from the active galactic nuclei detected.

Finally, the release of rotational kinetic energy does not contradict the fact that neither matter nor radiation can leave a black hole. Under certain conditions, the energy of a matter and/or radiation crossing the event horizon can be negative, which should lead to a decrease in the total energy of a black hole.

4.2. Black Hole as Unipolar Inductor

A unipolar inductor, which consists of a rotating magnetized object connected at two ends can be realized in nature by a rotating black hole in a test magnetic field which may lead to loss of the kinetic energy of rotation. A non-zero potential difference U is generated between the ends of the rotating object, which is the source of the electric current. Perfect conductor moving with the speed $\vec{v} = \vec{\Omega} \times \vec{r}$ in magnetic field, where Ω is angular velocity of rotation, $\vec{A}$ generates an induced electric field $\vec{E} = -\vec{v} \times \vec{B}/c$. Accordingly, the potential difference $U \sim ER$ at the ends of the rotating object with radius R is equal to

$$U \sim \frac{\Omega R}{c} R B_0 \,. \tag{2}$$

B_0 is the surface magnetic field.

It is the way how the kinetic energy of rotation is released from rotating magnetized neutron stars observed as radio pulsars where the spin down, i.e., rotation retardation mechanism is associated with surface currents closing electric currents flowing outside the magnetized neutron star. Energy will be carried away from the stellar surface by the flow of the Poynting vector $\vec{S}_P = (c/4\pi)\vec{E} \times \vec{B}$.

The exact expression for the charge density has the form

$$\rho_e = -\frac{(\vec{\Omega} \cdot \vec{B})}{2\pi c} \,. \tag{3}$$

Now multiplying the charge density ρ_e to the speed of light c, as well as to surface πR_0^2, where R_0 is transverse dimension of the area in which current I flows, one may get

$$I \sim \pi R_0^2 \rho_e c \,. \tag{4}$$

The total energy loss takes the form $W = IU$.

The well-known expression for the energy loss of radio pulsars is

$$W \sim \left(\frac{\Omega R_0}{c}\right)^2 B_0^2 R_0^2 c = \left(\frac{\Omega R}{c}\right)^4 B_0^2 R^2 c \,. \tag{5}$$

4.3. Black Hole in External Magnetic Field

A charged black hole has a radial electric field $E_r = Q/r^2$ where Q defines the electric charge of the black hole. A rotating charged black hole additionally generates a dipolar magnetic field

$$B^{\hat{r}} = (2QJ/M)r^{-3}\cos\theta \,, \quad B^{\hat{\theta}} = (QJ/M)r^{-3}\sin\theta \,, \tag{6}$$

where $Q\vec{J}/M$ is magnetic moment of a black hole.

However, the case of a charged black hole is not of practical interest. It is obvious that electrostatic forces, which are much superior to gravitational ones, quickly pump charges of the opposite sign from the environment to neutralize the charge Q of the black hole. For this reason, it is believed that the resulting black hole does not have its own intrinsic magnetic moment.

It is well understood how the magnetic moment of an uncharged, but initially magnetized star disappears during its gravitational collapse. This problem was first solved by Ginzburg (1964) (see also Ginzburg and Ozernoy (1964) for the case of a non-rotating collapsing star). The amplification of the surface magnetic field under the action of compression ($B \sim R^{-2}$) is held for relativistic neutron stars.

Assume R_0 and μ_0 are the initial radii and magnetic moment of a sphere contracting under the influence of gravity, respectively. In the nonrelativistic approximation, the magnetic moment μ ($\sim BR^3$) decreases as

$$\vec{\mu} = \vec{\mu}_0(R/R_0) \,, \tag{7}$$

i.e., $\mu \to 0$ at $R \to 0$. In general relativity, subject to freezing $B \sim R^{-2}$ also respected locally. However, the curvature has a significant global impact, and

$$\vec{\mu} = \vec{\mu}_0 2M/[3R_0 \ln(1-2M/R)] \,. \tag{8}$$

Now $\mu \to 0$ at $R \to r_g$. Given the dependence of the radius on time, for a remote external observer, the magnetic moment of a collapsing star decreases as t^{-1}. The magnetic field has the form

$$B^{\hat{r}} = 2\mu r^{-3}\cos\theta f(r) \,, \quad B^{\hat{\theta}} = \mu r^{-3}\sin\theta\psi(r) \,, \tag{9}$$

where the functions $f(r)$ and $\psi(r) \to 1$ at $r \gg r_g$ and at $r \to r_g$ are

$$f(r) \simeq -3\ln(1-2M/r) \,, \quad \psi(r) \simeq 3\ln(1-2M/r)^{-1/2} \,. \tag{10}$$

Consequently, the magnetic field damps by itself near the critical surface of the collapsing object ($B^{\hat{r}} \gg B^{\hat{\theta}}, r \to r_g$), however, the field decays with time for any given radius.

Kerr space-time exterior to a rapidly rotating compact astrophysical object in a spherical coordinate system (ct, r, θ, ϕ) is described by the metric

$$\begin{aligned} ds^2 = &-\tfrac{1}{\Sigma}(\Delta - a^2\sin^2\theta)dt^2 - \tfrac{4aMr\sin^2\theta}{\Sigma}dtd\varphi \\ &+\tfrac{1}{\Sigma}[(r^2+a^2)^2 - \Delta a^2\sin^2\theta]\sin^2\theta d\varphi^2 + \tfrac{\Sigma}{\Delta}dr^2 + \Sigma d\theta^2 \,, \end{aligned} \tag{11}$$

where parameters Σ and Δ are defined as

$$\Sigma = r^2 + a^2\cos^2\theta \,, \quad \Delta = r^2 - 2Mr + a^2 \tag{12}$$

$a = J/M$ is the specific angular momentum of a source with a total mass M.

The electromagnetic field of various black holes embedded in the external magnetic field is widely discussed in the literature (see e.g., [62–64]. The existence in the spacetime of time-like $\xi^{\alpha}_{(t)}$ and space-like $\xi^{\alpha}_{(\phi)}$ Killing vectors being responsible for the stationarity and axial symmetry of the geometry, respectively, and also satisfy the Killing equation

$$\xi_{\alpha;\beta} + \xi_{\beta;\alpha} = 0\,. \tag{13}$$

Therefore, the wave equations (in the vacuum space-time) have the form

$$\Box\xi^{\alpha} = 0\,, \tag{14}$$

which gives the right to choose the solution of Maxwell's vacuum equations in the Lorentz gauge for the vector potential A_{μ} of the electromagnetic field in a simple form

$$A^{\alpha} = C_1\xi^{\alpha}_{(t)} + C_2\xi^{\alpha}_{(\phi)}\,. \tag{15}$$

The constant $C_2 = B/2$, if the gravitational source is located in an asymptotically uniform magnetic field B , directed parallel to the axis of rotation. Constant value C_1 can be easily calculated from the asymptotic properties of space-time (11) at infinity.

To find a constant C_1 in Equation (15), one can use the condition of electrical neutrality of the source

$$\begin{array}{l} 4\pi Q = 0 = \frac{1}{2}\oint F^{\alpha\beta}{}_{*}dS_{\alpha\beta} = \\ C_1\oint\Gamma^{\alpha}_{\beta\gamma}u_{\alpha}m^{\beta}\xi^{\gamma}_{(t)}(uk)dS + \frac{B}{2}\oint\Gamma^{\alpha}_{\beta\gamma}u_{\alpha}m^{\beta}\xi^{\gamma}_{(\phi)}(uk)dS\,, \end{array} \tag{16}$$

estimating the magnitude of the integral over a spherical surface at asymptotic infinity. Here equality was used $\xi_{\beta;\alpha} = -\xi_{\alpha;\beta} = -\Gamma^{\gamma}_{\alpha\beta}\xi_{\gamma}$, following from the Killing equation, an element of an arbitrary 2-surface $dS^{\alpha\beta}$ presented as

$$dS^{\alpha\beta} = -u^{\alpha}\wedge m^{\beta}(uk)dS + \eta^{\alpha\beta\mu\nu}u_{\mu}n_{\nu}\sqrt{1+(uk)^2}dS\,. \tag{17}$$

The following expressions

$$\begin{array}{l} m_{\alpha} = \dfrac{\eta_{\lambda\alpha\mu\nu}u^{\lambda}n^{\mu}k^{\nu}}{\sqrt{1+(uk)^2}}, \quad n_{\alpha} = \dfrac{\eta_{\lambda\alpha\mu\nu}u^{\lambda}k^{\mu}m^{\nu}}{\sqrt{1+(uk)^2}}, \\ k^{\alpha} = -(uk)u^{\alpha} + \sqrt{1+(uk)^2}\eta^{\mu\alpha\rho\nu}u_{\mu}m_{\rho}n_{\nu}\,, \end{array} \tag{18}$$

related the three $k_{\alpha}, m_{\alpha}, n_{\alpha}$ space-like vectors. Normal vector n^{α} is orthogonal to two-surface, vector m^{α} belongs to a given two-surface, and the four-velocity of observer u^{α} is orthogonal to it. Space-like vector k^{α} is orthogonal to m^{α} and belongs to the surface. Here, dS is invariant surface element, $\wedge$ denotes an external product, $_{*}$ denotes dual element, $\eta_{\alpha\beta\gamma\delta}$ is pseudo-tensor expression of the Levi-Civita symbol $\epsilon_{\alpha\beta\gamma\delta}$.

Then inserting $u_0 = -(1-M/r)$, $m^1 = (1-M/r)$, as well as the values of the Christoffel symbols $\Gamma^0_{10} = M/r^2$ è $\Gamma^0_{13} = -J\sin^2\theta/r^2$ in asymptotics into expression (16) for flux, one may get the value of constant $C_1 = aB$.

The energetic activity of rotating magnetized neutron stars observed as radio pulsars due to the transformation of the kinetic energy of rotation into electromagnetic radiation could be treated as a common mechanism applicable to a rapidly rotating black hole. Therefore

(i) the presence of an external magnetic field playing the role of conducting wires,

(ii) the rapid rotation of the central black hole creating the potential difference U at the event horizon, and

(iii) generation of an electric current I, which carries energy from a rapidly rotating black hole and reduces the kinetic energy of rotation of the central black holeplays a key role to extract energy from BHs.

The nature of the energetic activity of a gravitational compact object is related to the problem of finding the structure of electric currents flowing in the plasma magnetosphere based on two important assumptions. On one side, it is assumed that the magnetic field is sufficiently large and can play the role of a conducting wire (this issue is also relevant to the plasma magnetosphere of magnetized neutron stars observed ad radio pulsars). On the other hand, the density of the medium is sufficiently small (so that the mean free path of the particles becomes greater than the radius of the circle $r_L = mcv/(eB)$ along which the charged particle moves in the magnetic field), and the radius r_L, will be much smaller than the size of the system, then, in this case, the conductivity of the medium across the magnetic field should be substantially suppressed. As a result, one can assume with high accuracy that a charged particle, and, therefore, an electric current, will only move along an external magnetic field.

4.4. Extracting Energy from Rapidly Rotating Black Holes: Blandford-Znajek Process

The mechanism of a unipolar inductor for a rotating sphere in the applied magnetic field can be directly applied to the magnetosphere of the rotating black hole. Blandford and Znajek in 1977 have first shown that a rotating black hole immersed in an external magnetic field can work as a unipolar inductor. It is apparent that energy losses for the rotating black hole can be evaluated similarly to the pulsar magnetosphere. However, the radius of the polar cap R_0 of the magnetized neutron star is substituted with the gravitational radius r_h of the event horizon. On the contrary to the rotating neutron star, because, unlike radio pulsars, the plasma rotation velocity is different from the angular velocity of rotation of the central compact object. Consequently, due to this difference, the black hole horizon can provide electromagnetic potential difference which can create flowing electric current $\vec{J}_H$ as in the classical unipolar inductor. The energy taken away by the electric currents can be written as $W = IU$ which in turn provides the expression

$$W_{BZ} \sim \left(\frac{\Omega r_g}{c}\right)^2 B_0^2 r_g^2 c\,, \tag{19}$$

derived in 1977 by Blandford and Znajek [65] when they treated the structure of the plasma magnetosphere of a rotating black hole. For active galactic nuclei with the typical values of parameters (for magnetic field $B_0 \sim 10^4$ G, the radius of black hole's event horizon $r_h \sim 10^{14}$ cm, $\Omega r_h/c \sim 1$), the derived simple formula is in good agreement with the observed energy loss $W \sim 10^{45}$ erg/s.

At the same time, despite the widespread use of the Blandford-Znajek mechanism to explain the nature of the activity of various astrophysical objects, the very possibility of electromagnetic energy release by a rotating black hole has been questioned for many years. In 1982, Thorne and MacDonald developed a novel approach that fully incorporated the formalism of the plasma magnetosphere of a neutron star to a rotating black hole. Close to the event horizon of a rotating black hole the concept of a conducting membrane was introduced with properties similar to magnetized neutron stars. It was demonstrated that the expression (19) for the energy loss of a rotating black hole can be associated with the braking effect of the Ampere force produced by the surface electric currents.

Such good agreement in the numbers is usually treated as a realistic confirmation of the efficiency of the Blandford-Znajek process for energy extraction from a rotating black hole. It is not requested for the charged particles to leave the black hole to close the electric current. The most important is that the total electric charge crossing the event horizon of the black hole vanishes. The far observer would detect the apparent result that any electric charges near the horizon are at the center of a black hole. It indicates that the surface electric currents are not important in black hole electrodynamics.

However, the generation of electromotive force by the Kerr black hole is due to the dragging of inertial frames (the effect of entrainment of reference systems), that is, with the appearance of gravitational magnetic forces.

The mechanism of energy release of relativistic compact objects is now correctly understood. Despite the fact that a rotating black hole immersed in an external magnetic field can indeed act as a unipolar inductor, the rotation retardation mechanism itself is not related to electric currents flowing along the surface of the black hole.

4.5. The Most Efficient Mechanism for the Energy Extraction from the Black Hole: Magnetic Penrose Process

As already emphasized, a plasma production mechanism should exist for the electric currents to flow in the magnetosphere of a rotating black hole to play a role of a unipolar inductor. Similar to the Penrose effect, one particle should fall into a black hole, and the second one should go to infinity. Accordingly, the Magnetic Penrose process to be discussed here is an electromagnetic implementation of the classical Penrose process. It is related to the charged test particles and the electromagnetic field produced by them.

Black holes have been proposed as a potential source of ultra-high-energy cosmic rays through a novel and highly efficient mechanism called the magnetic Penrose process. This process involves the extraction of electromagnetic energy from rotating black holes. The purpose of this description is to explore the potential of this mechanism for explaining the production of ultra-high-energy cosmic rays from supermassive black holes. We will begin by discussing key issues in black hole thermodynamics and reviewing important research related to energy extraction mechanisms from black holes.

Irreducible energy is evaluated at 71% of its total energy for the extreme Kerr black hole, while the rotational energy being available for extraction is estimated at the maximum limiting value of 29%. It is of order 10^{63} eV for the stellar mass astrophysical black holes, while this energy is of order 10^{74} eV for supermassive black holes (SMBHs) of mass $10^9 M_{\odot}$. This makes the SMBHs the largest energy reservoir in the Universe. Therefore it is important to explore the most effective and ultra-efficient ways of energy extraction from this enormous source. After analyzing the decay of an infalling particle into two fragments near a rotating black hole, it is possible to identify three different regimes of energy extraction from the black hole: low, moderate, and ultra. The efficiency of the process is defined as the ratio of the extracted energy to the infalling energy.

The process of interest is the magnetic Penrose process (MPP) [66–71]. When there is no magnetic field present, the MPP reverts to the original Penrose process, which provides a lower limit for the process. The maximum efficiency of the original Penrose process is 20.7%, which is achieved for an extreme Kerr (maximally rotating) black hole.

Our study, as outlined in reference [68], presents a graph showing the efficiency of energy extraction from the black hole as a function of rotation parameters for various values of the magnetic field. This can be seen in Figure 11. The efficiency continues to increase with increasing rotation parameters of the black hole until it reaches the point of extremality $a = M$, at which point it drops to the value of a pure Kerr black hole, this happens due to the fact that the magnetic field is expelled from the horizon. This phenomenon is a gravitational analog of the well-known Meissner effect in superconductors, in which the magnetic field is expelled as a conductor becomes superconducting. Therefore, for the most efficient energy extraction using MPP, the black hole should be near extremal but not exactly extremal.

The radiative efficiency is reduced to the expression $\eta_{MPP}^{mod.} = q_3/q_1 - 1$ in the case when all particles are electrically charged. This is the so-called moderate regime of MPP, which is operative if $q_3 > q_1$. Consequently, the gravitationally induced electric field of the black hole is neutralized. The main driving force behind the behavior of a Kerr black hole is the quadrupole electric field that is produced by the twisting of magnetic field lines due to the frame-dragging effect. There exists also the most efficient regime of MPP. When an electrically neutral infalling particle is split into two charged fragments within

the ergosphere, the efficiency of this process is primarily determined by the ratio of the charge of the smaller fragment to the mass of the larger fragment multiplied by the area of the horizon: $\eta_{MPP}^{ultra} = q_3/m_1 A_t$. For electrons and protons, this ratio is very high, resulting in extremely high-efficiency values. Even for relatively low magnetic field strengths on the order of a Gauss, this efficiency can exceed 100%. For electrons, this can happen at even lower magnetic field strengths, on the order of milliGauss.

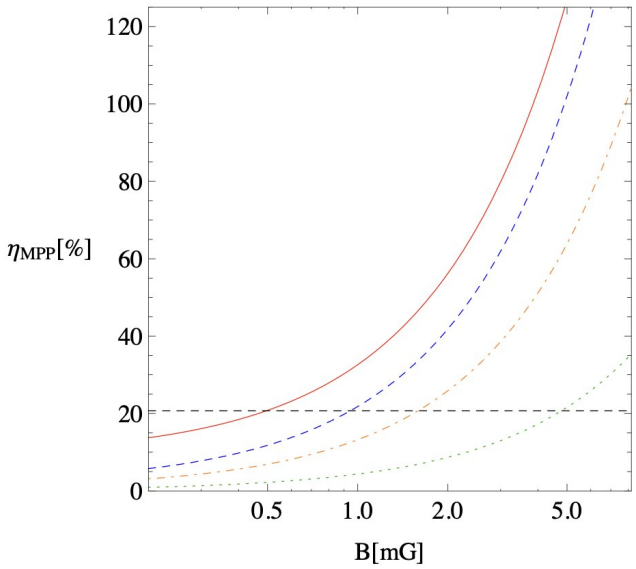

Figure 11. The graph displays the correlation between MPP efficiency and magnetic field strength. It includes data points for different values of the spin parameter a: $0.1M$ (represented by a dotted line), $0.3M$ (dot-dashed line), $0.5M$ (dashed line), $0.9M$ (solid line), and M (represented by a horizontal dashed line). The value of M is set to $10M_{\odot}$. For additional information, refer to the research paper [68].

Exploring the potential use of MPP in the ultra regime to understand the origin and production of ultra-high-energy cosmic rays (UHECR) is an exciting area of research. These particles are the most energetic ever detected on Earth, with energies $E > 10^{18}$ eV that far surpass those with maximum energy $\sim 10^{13}$ eV per beam that can be generated by the current most powerful particle accelerators, such as the LHC. The composition of UHECRs is thought to be a mix of extragalactic charged particles, although previous measurements have suggested that protons make up the majority of the flux. The spectrum of cosmic rays also shows features known as the "knee" and "ankle", with the knee at around $10^{15.5}$ eV generally attributed to Galactic supernova explosions. However, the significant decrease in flux between the knee and the ankle at around $10^{18.5}$ eV suggests that the source of these particles may be different.

Explanations for the highest-energy cosmic rays have been proposed, including theories involving extra dimensions, Lorentz invariance violations, and new exotic particles. While the acceleration of these particles through relativistic shocks in jets has been considered a likely possibility, recent research suggests that this mechanism cannot account for protons with energies above 10^{20} eV. Additionally, interactions with matter and light during their journey through space can greatly reduce the energies of these cosmic rays, leaving the question of their origins unresolved.

An alternate method of extracting kinetic energy from black holes, known as the magnetic Penrose process (MPP), could potentially provide an explanation for the origin of UHECRs. By analyzing the beta-decay of neutrons in the presence of a magnetic field near a supermassive black hole, it is possible to estimate the energy of the resulting protons. Using this method, protons with energies above 10^{20} eV can be produced due to the beta-decay defined by the relation $E_p = 1.33 \times 10^{20}\,\mathrm{eV}(q/e)$for a black hole with a mass of $10^9 M_{\odot}$ and a magnetic field of 10^4 G.

The process described here can be applied to any decay mode and results in a significant increase in the energy of the escaping particle. In realistic scenarios, the energy gain can be more than 10^{10} times that of the infalling particle, due to the large value of the parameter $qGBM/mc^4$, which is around 10^{11} for protons and 10^{14} for electrons around a supermassive black hole of $10^9 M_\odot$ and magnetic field strength of 10^4 G.

The ability to produce ultra-high energy particles through neutral particle ionization is not dependent on the specific configuration of the magnetic field. Instead, the presence of the A_t component of the electromagnetic field, which is generated by the rotation of the black hole, is crucial. While configurations with open field lines may appear more favorable for particle escape, particles that are accelerated to extremely high velocities may be able to cross the field lines and escape the black hole with deflections.

Testing the magnetic Penrose process (MPP) under different magnetic field configurations, it can be observed that the total energy of the escaping particle remains consistent regardless of the field configuration, while the direction of escape varies. For a uniform magnetic field, all escaping particles are collimated in the same direction, while for radial magnetic fields of a monopole character, the charged particles escape isotropically. Additionally, it is found that the initial energy and angular momentum of the incident-neutral particle do not significantly impact the acceleration of its charged fragments.

When primary cosmic rays travel through regions with strong magnetic fields, they can emit synchrotron radiation and lose energy. This effect is particularly pronounced in source regions where the magnetic fields are particularly strong. Our research has revealed that electrons lose energy at a rate that is 10^{10} times faster than protons in conditions similar to those found in the vicinity of supermassive black holes. As a result, for typical SMBH with a magnetic field of $B = 10^4$ G order, it is much more likely that primary cosmic rays in these regions are protons or ions, rather than electrons. This is because the energy loss rate for electrons is so high that they would not be able to escape from the vicinity of a black hole.

UHECRs, or ultra-high-energy cosmic rays, can lose a significant amount of energy through interactions with dense astrophysical matter, particularly in the environments of supermassive black holes. This can happen in various ways, such as through the Greisen–Zatsepin–Kuzmin cutoff (GZK-cutoff) and synchrotron emission. The movement of UHECRs produced by magnetic reconnection in plasma (MPP) is affected by chaotic scattering at the corresponding effective potential, causing them to escape along magnetic field lines. However, the direction of escape can be altered by magnetic reconnection events in strong gravity environments, leading the UHECRs to move out of dense accretion disks and jet-dominated regions. Alternatively, UHECRs resulting from highly efficient MPP can become part of jets, and the acceleration caused by both MPP and relativistic shocks in jets can be combined. In this scenario, MPP acts as a supplementary force in models of UHECR acceleration by relativistic shocks in plasma jets. Additionally, UHECRs produced through MPP can serve as indicators of secondary high-energy particles, such as neutrinos and gamma rays.

5. Conclusions

In this work, the investigation of electromagnetic, optical, and energetic properties of astrophysical and galactic black holes and the surrounding matter is reviewed. The astrophysical applications of the theoretical models of black hole environment to the description of various observed phenomena, such as black hole shadow, ultra-relativistic jets, quasiperiodic oscillations, and UHECRs, are discussed.

Here we emphasize and briefly summarize the results of reviewed research and describe the comprehensive conclusions which are deduced from the review. The scientific significance of the up-to-date research on black hole physics is usually treated by formalism to analyze the electromagnetic fields of astrophysical black holes, energy extraction mechanisms from astrophysical black holes, and determination of images of the black

holes observed by modern radiotelescopes, and extract essential data related to the main spacetime parameters being relevant to SMBHs located in the central part of most galaxies.

In GR Tashkent group the extensive study devoted to optical properties of astrophysical and SMBHs is performed [55,56]. A new TM code is recently developed to simulate the image of BH surrounded by an accretion disk. The example of the simulated image is presented in Figures 7 and 8. One can observe from Figure 8 that the simulated images obtained by using numerical TM code are in rough agreement with the experimental results obtained by the EHT collaboration. As the next step, we are planning to develop a code to make corresponding data fitting process to get constraints on black hole spacetime parameters with the more sensitive future data of EHT.

The surface brightness and spectra of the accretion disks through X-ray observations of black holes would give an opportunity to get constraints on the desired parameters of black holes and alternative theories of gravity. It may be important to the energetic activity of AGNs, quasars etc.

The recent triumphal discoveries related to BH observations with an increase in the accuracy of the measurements would provide constraints on different parameters of black holes such as mass, spin, orientation, charge, and magnetic field. The strong gravity regime can be tested through the development of advanced observational tools to extract distinguishable signatures for compact black hole alternatives.

Research on black holes and high-energy cosmic rays can provide insight into the properties of supermassive black holes like Sgr A* at the center of our galaxy, as well as the dynamics of the plasma surrounding them. Understanding the energy characteristics of black holes, practical techniques for extracting rotational energy via electromagnetic means, and high-energy processes are crucial areas of study.

The motion of photons and dynamics of the test particles in a black hole close vicinity, together with observed QPOs can play an important role as a relativistic laboratory to probe the main parameters of as total mass and spin of stellar-mass black holes and microquasars. The existence and justifications of compact black holes in nature could be provided through the study of the optical processes in the black hole environment.

The astronomical observation of black holes provides a rich fundamental physics laboratory for experimental tests and verification of black hole accretion models and various theories of gravity in the strong gravitational field regime. We expect revolutionary triumphal discoveries in the golden era of the study of black hole physics.

Author Contributions: Conceptualization, B.N. and B.A.; methodology, B.N. and B.A.; software, B.N.; data curation, B.N. and B.A.; writing—original draft preparation, B.N. and B.A.; formal analysis, B.N. and B.A.; supervision, B.A.; project administration, B.A. All authors have read and agreed to the published version of the manuscript.

Funding: This research is supported by Grants F-FA-2021-432 and MRB-2021-527 of the Uzbekistan Ministry for Innovative Development and by the AS-ICTP under the Grant No. OEA-NT-01.

Data Availability Statement: Not applicable

Acknowledgments: We thank Temurbek Mirzaev and Dilshodbek Bardiev for the simulated images of the SMBHs M87* and Sgr A*, and GRMHD simulations of torus around the the Schwarzshild black hole, respectively.

Conflicts of Interest: The authors declare no conflict of interest.

References

1. Alberdi, A.; Alef, W.; Asada, K.; Azulay, R.; Baczko, A.; Ball, D.; Baloković, M.; Barrett, J.; Bintley, D.; Blackburn, L.; et al. First M87 Event Horizon Telescope Results. I. The Shadow of the Supermassive Black Hole. *Astrophys. J. Lett.* **2019**, *875*, L1. [CrossRef]
2. Alberdi, A.; Alef, W.; Algaba, J.C.; Anantua, R.; Asada, K.; Azulay, R.; Bach, U.; Baczko, A.; Ball, D.; Baloković, M.; et al. First Sagittarius A* Event Horizon Telescope Results. I. The Shadow of the Supermassive Black Hole in the Center of the Milky Way. *Astrophys. J. Lett.* **2022**, *930*, L12. [CrossRef]
3. Narzilloev, B.; Malafarina, D.; Abdujabbarov, A.; Ahmedov, B.; Bambi, C. Particle motion around a static axially symmetric wormhole. *Phys. Rev. D* **2021**, *104*, 064016. [CrossRef]

4. Rayimbaev, J.; Narzilloev, B.; Abdujabbarov, A.; Ahmedov, B. Dynamics of Magnetized and Magnetically Charged Particles around Regular Nonminimal Magnetic Black Holes. *Galaxies* **2021**, *9*, 71. [CrossRef]
5. Narzilloev, B.; Rayimbaev, J.; Abdujabbarov, A.; Ahmedov, B. Regular Bardeen Black Holes in Anti-de Sitter Spacetime versus Kerr Black Holes through Particle Dynamics. *Galaxies* **2021**, *9*, 63. [CrossRef]
6. Narzilloev, B.; Shaymatov, S.; Hussain, I.; Abdujabbarov, A.; Ahmedov, B.; Bambi, C. Motion of Particles and Gravitational Lensing Around (2+1)-dimensional BTZ black holes in Gauss-Bonnet Gravity. *Eur. Phys. J. C* **2021**, *81*, 849. [CrossRef]
7. Narzilloev, B.; Hussain, I.; Abdujabbarov, A.; Ahmedov, B.; Bambi, C. Dynamics and fundamental frequencies of test particles orbiting Kerr–Newman–NUT–Kiselev black hole in Rastall gravity. *Eur. Phys. J. Plus* **2021**, *136*, 1032. [CrossRef]
8. Narzilloev, B.; Hussain, I.; Abdujabbarov, A.; Ahmedov, B. Optical properties of an axially symmetric black hole in the Rastall gravity. *Eur. Phys. J. Plus* **2022**, *137*, 645. [CrossRef]
9. Narzilloev, B.; Ahmedov, B. Radiation Properties of the Accretion Disk around a Black Hole Surrounded by PFDM. *Symmetry* **2022**, *14*, 1765. [CrossRef]
10. Narzilloev, B.; Ahmedov, B. Regular black hole solution in PFDM environment to explain the radiative efficiency of black hole candidates. *New Astron.* **2023**, *98*, 101922. [CrossRef]
11. Narzilloev, B.; Abdujabbarov, A.; Hakimov, A. Redshift of photons emitted from the accretion disk of a regular black hole surrounded by dark matter. *Int. J. Mod. Phys. A* **2022**, *37*, 2250144. [CrossRef]
12. Juraeva, N.; Rayimbaev, J.; Abdujabbarov, A.; Ahmedov, B.; Palvanov, S. Distinguishing magnetically and electrically charged Reissner–Nordström black holes by magnetized particle motion. *Eur. Phys. J. C* **2021**, *81*, 70. [CrossRef]
13. Bokhari, A.H.; Rayimbaev, J.; Ahmedov, B. Test particles dynamics around deformed Reissner-Nordström black hole. *Phys. Rev. D* **2021**, *102*, 124078. [CrossRef]
14. Rayimbaev, J.; Shaymatov, S.; Jamil, M. Dynamics and epicyclic motions of particles around the Schwarzschild–de Sitter black hole in perfect fluid dark matter. *Eur. Phys. J. C* **2021**, *81*, 699. [CrossRef]
15. Rayimbaev, J.; Tadjimuratov, P. Can modified gravity silence radio-loud pulsars? *Phys. Rev. D* **2020**, *102*, 024019. [CrossRef]
16. Fishbone, L.G.; Moncrief, V. Relativistic fluid disks in orbit around Kerr black holes. *Astrophys. J.* **1976**, *207*, 962–976. [CrossRef]
17. Novikov, I.D.; Thorne, K.S. Astrophysics and black holes. In *Les Houches Summer School of Theoretical Physics: Black Holes, Proceedings of the Ecole d'Eté de Physique Théorique, Les Astres Occlus, Les Houches, France, August, 1973*; Gordon and Breach: New York, NY, USA, 1973; pp. 343–550.
18. Page, D.N.; Thorne, K.S. Disk-Accretion onto a Black Hole. Time-Averaged Structure of Accretion Disk. *Astrophys. J.* **1974**, *191*, 499–506. [CrossRef]
19. Banerjee, I.; Chakraborty, S.; SenGupta, S. Decoding signatures of extra dimensions and estimating spin of quasars from the continuum spectrum. *Phys. Rev. D* **2019**, *100*, 044045. [CrossRef]
20. Zhang, S.N.; Cui, W.; Chen, W. Black Hole Spin in X-Ray Binaries: Observational Consequences. *Astrophys. J.* **1997**, *482*, L155–L158. [CrossRef]
21. Bambi, C. A Code to Compute the Emission of Thin Accretion Disks in Non-Kerr Spacetimes and Test the Nature of Black Hole Candidates. *Astrophys. J.* **2012**, *761*, 174. [CrossRef]
22. Kong, L.; Li, Z.; Bambi, C. Constraints on the Spacetime Geometry around 10 Stellar-Mass Black Hole Candidates from the Disk's Thermal Spectrum. *Astrophys. J.* **2014**, *797*, 78. [CrossRef]
23. McClintock, J.E.; Narayan, R.; Steiner, J.F. Black Hole Spin via Continuum Fitting and the Role of Spin in Powering Transient Jets. *Space Sci. Rev.* **2014**, *183*, 295–322. [CrossRef]
24. McClintock, J.E.; Narayan, R.; Davis, S.W.; Gou, L.; Kulkarni, A.; Orosz, J.A.; Penna, R.F.; Remillard, R.A.; Steiner, J.F. Measuring the spins of accreting black holes. *Class. Quantum Gravity* **2011**, *28*, 114009. [CrossRef]
25. Czerny, B.; Hryniewicz, K.; Nikolajuk, M.; Sadowski, A. Constraints on the black hole spin in the quasar SDSS J094533.99+100950.1. *Mon. Not. R. Astron. Soc.* **2011**, *415*, 2942. [CrossRef]
26. Done, C.; Jin, C.; Middleton, M.; Ward, M. A new way to measure supermassive black hole spin in accretion disc-dominated active galaxies. *Mon. Not. R. Astron. Soc.* **2013**, *434*, 1955–1963. [CrossRef]
27. Nampalliwar, S.; Bambi, C. Accreting Black Holes. In *Tutorial Guide to X-ray and Gamma-ray Astronomy: Data Reduction and Analysis*; Bambi, C., Ed.; Springer: Singapore, 2020; pp. 15–54. [CrossRef]
28. Risaliti, G.; Harrison, F.; Madsen, K.; Walton, D.; Boggs, S.; Christensen, F.; Craig, W.; Grefenstette, B.; Hailey, C.; Nardini, E.; et al. A rapidly spinning supermassive black hole at the centre of NGC 1365. *Nature* **2013**, *494*, 449–451. [CrossRef]
29. Remillard, R.A.; McClintock, J.E. X-ray Properties of Black-Hole Binaries. *Ann. Rev. Astron. Astrophys.* **2006**, *44*, 49–92. [CrossRef]
30. van der Klis, M. A Review of Rapid X-ray Variability in X-ray Binaries. *arXiv* **2004**, arXiv:astro-ph/0410551.
31. Stella, L.; Vietri, M. Lense-Thirring precession and QPOs in low mass X-ray binaries. *Nucl. Phys. B Proc. Suppl.* **1999**, *69*, 135–140. [CrossRef]
32. Stella, L.; Vietri, M. kHz Quasiperiodic Oscillations in Low-Mass X-Ray Binaries as Probes of General Relativity in the Strong-Field Regime. *Phys. Rev. Lett.* **1999**, *82*, 17–20. [CrossRef]
33. Stella, L.; Vietri, M.; Morsink, S.M. Correlations in the Quasi-periodic Oscillation Frequencies of Low-Mass X-Ray Binaries and the Relativistic Precession Model. *Astrophys. J.* **1999**, *524*, L63–L66. [CrossRef]
34. Abramowicz, M.A.; Karas, V.; Kluzniak, W.; Lee, W.H.; Rebusco, P. Nonlinear resonance in nearly geodesic motion in low mass x-ray binaries. *Publ. Astron. Soc. Jap.* **2003**, *55*, 466–467. [CrossRef]

35. Abramowicz, M.A.; Kluzniak, W. A Precise determination of angular momentum in the black hole candidate GRO J1655-40. *Astron. Astrophys.* **2001**, *374*, L19. [CrossRef]
36. Kluzniak, W.; Abramowicz, M.A. The physics of kHz QPOs—Strong gravity's coupled anharmonic oscillators. *arXiv* **2001**, arXiv:astro-ph/0105057.
37. Perez, C.A.; Silbergleit, A.S.; Wagoner, R.V.; Lehr, D.E. Relativistic diskoseismology. 1. Analytical results for 'gravity modes'. *Astrophys. J.* **1997**, *476*, 589–604. [CrossRef]
38. Silbergleit, A.S.; Wagoner, R.V.; Ortega-Rodríguez, M. Relativistic Diskoseismology. II. Analytical Results for c-modes. *Astrophys. J.* **2001**, *548*, 335–347.
39. Wagoner, R.V.; Silbergleit, A.S.; Ortega-Rodríguez, M. "Stable" Quasi-periodic Oscillations and Black Hole Properties from Diskoseismology. *Astrophys. J.* **2001**, *559*, L25–L28. [CrossRef]
40. Bambi, C., Quasi-periodic Oscillations. In *Black Holes: A Laboratory for Testing Strong Gravity*; Springer: Singapore, 2017; pp. 181–192. [CrossRef]
41. Motta, S.E.; Belloni, T.M.; Stella, L.; Muñoz-Darias, T.; Fender, R. Precise mass and spin measurements for a stellar-mass black hole through X-ray timing: The case of GRO J1655-40. *Mon. Not. R. Astron. Soc.* **2013**, *437*, 2554–2565. [CrossRef]
42. Kato, S. A Resonantly Excited Disk-Oscillation Model of High-Frequency QPOs of Microquasars. *Publ. Astron. Soc. Jpn.* **2012**, *64*, 139. [CrossRef]
43. Abramowicz, M.A.; Kluzniak, W.; Stuchlik, Z.; Torok, G. The Orbital resonance model for twin peak kHz QPOs: Measuring the black hole spins in microquasars. *arXiv* **2004**, arXiv:aastro-ph/0401464.
44. Rayimbaev, J.; Abdujabbarov, A.; Abdulkhamidov, F.; Khamidov, V.; Djumanov, S.; Toshov, J.; Inoyatov, S. Quasiperiodic oscillation around charged black holes in Einstein–Maxwell-scalar theory. *Eur. Phys. J. C* **2022**, *82*, 1110. [CrossRef]
45. Rayimbaev, J.; Pantig, R.C.; Övgün, A.; Abdujabbarov, A.; Demir, D. Quasiperiodic oscillations, weak field lensing and shadow cast around black holes in Symmergent gravity. *arXiv* **2022**, arXiv:gr-qc/2206.06599.
46. Rayimbaev, J.; Bokhari, A.H.; Ahmedov, B. Quasiperiodic oscillations from noncommutative inspired black holes. *Class. Quant. Grav.* **2022**, *39*, 075021. [CrossRef]
47. Rayimbaev, J.; Majeed, B.; Jamil, M.; Jusufi, K.; Wang, A. Quasiperiodic oscillations, quasinormal modes and shadows of Bardeen–Kiselev Black Holes. *Phys. Dark Univ.* **2022**, *35*, 100930. [CrossRef]
48. Rayimbaev, J.; Bardiev, D.; Abdujabbarov, A.; Turaev, Y.; Stuchlík, Z. Quasi-periodic oscillation around regular Bardeen black holes in 4D Einstein–Gauss–Bonnet gravity. *Int. J. Mod. Phys. D* **2022**, *31*, 2250004. [CrossRef]
49. Bardeen, J. Non-singular general-relativistic gravitational collapse. In Proceedings of the International Conference GR5, New York, NY, USA, 9–13 September 1968; DeWitt, C., DeWitt, B., Eds.; Gordon and Breach: Tbilisi, Georgia, 1968; p. 174.
50. Luminet, J.P. Image of a spherical black hole with thin accretion disk. *Astron. Astrophys.* **1979**, *75*, 228–235.
51. Falcke, H.; Melia, F.; Agol, E. Viewing the Shadow of the Black Hole at the Galactic Center. *Astrophys. J.* **2000**, *528*, L13–L16. [CrossRef]
52. Chan, C.k.; Psaltis, D.; Özel, F. GRay: A Massively Parallel GPU-based Code for Ray Tracing in Relativistic Spacetimes. *Astrophys. J.* **2013**, *777*, 13. [CrossRef]
53. Bambi, C. Imaging Black Holes. In *Black Holes: A Laboratory for Testing Strong Gravity*; Springer: Singapore, 2017; pp. 193–205. [CrossRef]
54. Abdujabbarov, A.A.; Rezzolla, L.; Ahmedov, B.J. A coordinate-independent characterization of a black hole shadow. *Mon. Not. R. Astron. Soc.* **2015**, *454*, 2423–2435. [CrossRef]
55. Ahmedov, B. Development and perspectives of relativistic astrophysics in Uzbekistan. *Arab. J. Math.* **2022**, *11*, 141–153. [CrossRef]
56. Ahmedov, B. Relativistic Astrophysics in Uzbekistan. In *Under One Sky: The IAU Centenary Symposium*; Sterken, C., Hearnshaw, J., Valls-Gabaud, D., Eds.; Cambridge University Press: Cambridge, UK, 2019; Volume 349, pp. 276–282. [CrossRef]
57. Merritt, D. *Dynamics and Evolution of Galactic Nuclei*; Princton University Press: Princeton, NJ, USA, 2013.
58. Turimov, B.; Ahmedov, B.; Abdujabbarov, A.; Bambi, C. Gravitational lensing by a magnetized compact object in the presence of plasma. *Int. J. Mod. Phys. D* **2019**, *28*, 2040013. [CrossRef]
59. Toshmatov, B.; Stuchlík, Z.; Schee, J.; Ahmedov, B. Electromagnetic perturbations of black holes in general relativity coupled to nonlinear electrodynamics. *Phys. Rev. D* **2018**, *97*, 084058. [CrossRef]
60. Salpeter, E.E. Accretion of Interstellar Matter by Massive Objects. *Astrophys. J.* **1964**, *140*, 796–800. [CrossRef]
61. Zeldovich, Y.; Novikov, I. Doklady Akademii Nauk. *SSSR* **1964**, *158*, 811.
62. Wald, R.M. Black hole in a uniform magnetic field. *Phys. Rev. D* **1974**, *10*, 1680–1685. [CrossRef]
63. Aliev, A.N.; Özdemir, N. Motion of charged particles around a rotating black hole in a magnetic field. *Mon. Not. R. Astron. Soc.* **2002**, *336*, 241–248. [CrossRef]
64. Aliev, A.N.; Frolov, V.P. Five-dimensional rotating black hole in a uniform magnetic field: The gyromagnetic ratio. *Phys. Rev. D* **2004**, *69*, 084022. [CrossRef]
65. Blandford, R.D.; Znajek, R.L. Electromagnetic extraction of energy from Kerr black holes. *Mon. Not. R. Astron. Soc.* **1977**, *179*, 433–456. [CrossRef]
66. Tursunov, A.; Stuchlík, Z.; Kološ, M.; Dadhich, N.; Ahmedov, B. Supermassive Black Holes as Possible Sources of Ultrahigh-energy Cosmic Rays. *Astrophys. J.* **2020**, *895*, 14. [CrossRef]

67. Stuchlík, Z.; Kološ, M.; Tursunov, A. Penrose Process: Its Variants and Astrophysical Applications. *Universe* **2021**, *7*, 416. [CrossRef]
68. Dadhich, N.; Tursunov, A.; Ahmedov, B.; Stuchlík, Z. The distinguishing signature of magnetic Penrose process. *Mon. Not. R. Astron. Soc.* **2018**, *478*, L89–L94. [CrossRef]
69. Tursunov, A.; Dadhich, N. Fifty Years of Energy Extraction from Rotating Black Hole: Revisiting Magnetic Penrose Process. *Universe* **2019**, *5*, 125. [CrossRef]
70. Kološ, M.; Tursunov, A.; Stuchlík, Z. Radiative Penrose process: Energy gain by a single radiating charged particle in the ergosphere of rotating black hole. *Phys. Rev. D* **2021**, *103*, 024021. [CrossRef]
71. Stuchlík, Z.; Kološ, M.; Kovář, J.; Slaný, P.; Tursunov, A. Influence of Cosmic Repulsion and Magnetic Fields on Accretion Disks Rotating around Kerr Black Holes. *Universe* **2020**, *6*, 26. [CrossRef]